TECHNICAL UNIVERSITY OF LIBEREC
Faculty of Mechatronics, Informatics
and Interdisciplinary Studies

Control of Continuous Casting Process Based on Two-Dimensional Flow Field Measurements

Doctoral Thesis Summary

Liberec 2022

Abstract

Two-dimensional flow field measurement allows us to obtain detailed information about the processes inside the continuous casting mould. This is very important because the flow phenomena in the mould are complex, and they significantly affect the steel quality. For this reason, control based on two-dimensional flow monitoring has a great potential to achieve substantial improvement over the conventional continuous casting control. This conventional control relies on single-point measurements of selected scalar variables; typically, it is limited to mould level control. Two-dimensional flow field measurement provides large amounts of measurement data distributed within the whole cross-section of the mould. Such data can be obtained using process tomography or other sensors with similar distributed measurement capacity.

An experimental setup of the continuous casting process called Mini-LIMMCAST located in Helmholtz-Zentrum Dresden-Rossendorf (HZDR), Dresden, Germany, is used for this thesis. The mini-LIMMCAST facility is a small-scale physical model of a continuous caster working with a eutectic GaInSn alloy at room temperature. This thesis examines two alternatives of flow measurement sensors: Ultrasound Doppler Velocimetry (UDV) and Contactless Inductive Flow Tomography (CIFT). Both sensor variants can obtain information on the velocity profile in the mould.

Available literature sporadically mentions the use of tomographic or similar sensors for real-time feedback control of various processes. However, the field of tomography-based control is still very young. Therefore, this thesis explores various approaches for utilizing the large amounts of data such sensors provide for automatic control. Generally, model-based approaches were preferred for the design of controllers whose objective is to achieve optimal flow patterns in the mould.

Two approaches were considered to create the process model needed for model-based control: a spatially discretized version of a model based on partial differential equations and computational fluid dynamics and a model obtained using system identification methods. In the end, system identification proved to be more fruitful for the aim of creating the model-based controller. Specific features of the flow were parametrized to obtain the needed controlled variables and outputs of identified models. These features are mainly related to the exiting jet angle and the meniscus velocity. The manipulated variables considered are electromagnetic brake current and stopper rod position. Model predictive control in several versions was used as the main control approach, and the results of simulation experiments demonstrate that the model predictive controller can control the flow and achieve the optimum flow structures in the mould using UDV. CIFT measurements can provide similar velocity profiles. However, further technical developments in the CIFT sensor signal processing, such as compensating for the effects

of the strong and time-varying magnetic field of the electromagnetic brake on CIFT measurements, are necessary if this sensor is to be used for closed-loop control.

Abstrakt

Za pomoci dvourozměrného měření pole proudění v krystalizátoru zařízení pro plynulé lití oceli lze získat podrobnou informaci o procesech, které tam probíhají. Tato informace je velmi důležitá, neboť složitá struktura proudění v krystalizátoru výrazným způsobem ovlivňuje kvalitu lité oceli. Z tohoto důvodu má zpětnovazební řízení založené na takovémto dvourozměrném měření velký potenciál k tomu, aby dosáhlo výrazného zlepšení oproti obvyklým postupům řízení procesu plynulého lití. Tyto postupy totiž vycházejí pouze z bodového měření vybraných skalárních veličin a základní regulační smyčkou je obvykle řízení výšky hladiny v krystalizátoru.

Dvourozměrné měření pole proudění v krystalizátoru poskytuje velké množství naměřených hodnot, které jsou rozloženy v celém průřezu krystalizátoru. Technicky může být takovéto měření realizováno pomocí průmyslové tomografie nebo jiných snímačů, které jsou podobně jako tomografie schopné snímat veličiny rozložené v rámci celého průřezu krystalizátoru. V práci je jako zdroj experimentálních dat použito zařízení Mini-LIMMCAST provozované v Helmholtz-Zentrum Dresden-Rossendorf (HZDR). Toto zařízení představuje malý model procesu plynulého lití pracující s eutektickou slitinou GaInSn, která umožňuje provádění experimentů za pokojové teploty. K měření dvourozměrného pole proudění v krystalizátoru jsou alternativně používány snímače založené na dvou různých principech: ultrazvuková dopplerovská velocimetrie (Ultrasound Doppler Velocimetry - UDV) a bezkontaktní induktivní průtoková tomografie (Contactless Inductive Flow Tomography - CIFT). Z obou variant snímačů lze získat informaci o rychlostním poli proudění v krystalizátoru.

V dostupné literatuře lze najít občasné zmínky o použití průmyslových tomografických a obdobných snímačů pro zpětnovazební řízení různých procesů. Vcelku se však jedná o problematiku, jejíž výzkum je teprve v počátcích. V rámci práce bylo nutné se zabývat volbou a výzkumem vhodných metod automatického řízení, které umožňují využít rozsáhlé množství dat, které tyto snímače poskytují. Při návrhu metod řízení schopných zabezpečit, že proudění v krystalizátoru bude optimální z hlediska kvality výsledného produktu, byly v zásadě preferovány přístupy založené na modelu.

Pro vytvoření modelu byly zvažovány dva základní přístupy: jednak prostorově diskretizovaná podoba modelu založeného na parciálních diferenciálních rovnicích a výpočetní dynamice tekutin a jednak model získaný postupy identifikace systémů. Tento druhý přístup se ukázal pro realizaci řízení založeného na modelu jako výrazně vhodnější. Z dat byly extrahovány vhodné numerické charakteristiky proudění v krystalizátoru (úhel proudění z ponorné trysky, rychlost proudění na hladině krystalizátoru a další), které bylo možné použít jako regulované veličiny a výstupy modelů získaných identifikací. Jako akční veličiny byly použity proud elektromagnetické brzdy a poloha regulovatelné výpusti z mezipánve. Hlavním přístupem k řízení v práci jsou různé verze prediktivního řízení

založeného na modelu. Ve spojení s UDV snímači byly navržené prediktivní regulátory schopné dosáhnout v simulačních experimentech stanoveného cíle řízení a zabezpečit optimální struktury proudění v krystalizátoru. CIFT snímače jsou v principu schopné poskytnout podobná data, nicméně pro jejich využití pro řízení v uzavřené smyčce bude nezbytný další výzkum v oblasti vyhodnocení signálu z těchto snímačů, kde je otevřeným problémem kompenzace vlivu silného proměnného magnetického pole elektromagnetické brzdy na signál z těchto snímačů.

Table of Contents

1. Continuous Casting Process

Continuous casting is a vital process that accounts for approximately 95 percent of global steel production [1]. Figure 1.1 depicts the main operation of a continuous caster in which liquid steel flows from the ladle to the tundish and then into the mould through a submerged entry nozzle (SEN). A stopper rod or a sliding gate regulates the flow rate [2]. A solid steel shell is formed in the water-cooled mould, and the partially solidified strand is transported on rolls and cooled by water sprays until it is completely solidified. Additionally, argon gas is injected into the SEN for several steel grades to prevent nozzle clogging and to float inclusions. If argon is used, the flow field in the mould must not obstruct the rise of bubbles to the free surface[3]–[5].

The flow regime in the SEN and in the mould has a significant influence on the final product's quality. Issues such as clogging, turbulent flow, deep penetration of the jet, and slag entrapment have been shown to have a detrimental effect on the quality of the steel [4], [6]–[8]. The following sections will demonstrate that the challenge of controlling the continuous casting process is limited not only by the need to accurately model the process, but also by the sensors used in the process. This is where two-dimensional flow monitoring comes into play as these sensors are able provide us with richer data that can be utilized for control.
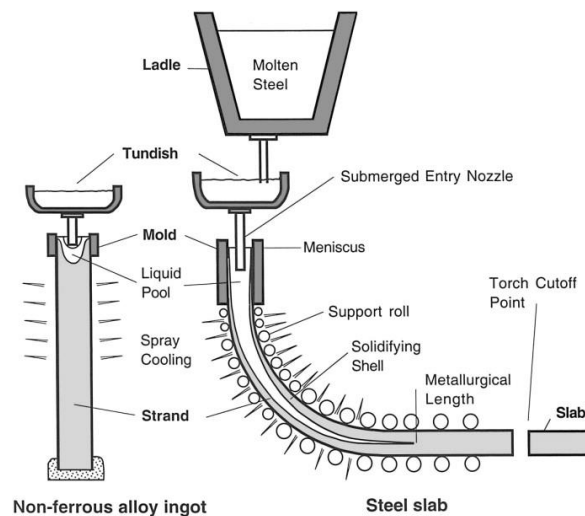
Figure 1.1. Schematic diagram of the continuous casting process [8]

1.1. Control of Continuous Caster

1.1.1. Mould Level

There is very little research on the use of two-dimensional flow field measurements in continuous caster control; most of the current research is based on conventional sensors

and knowledge about the relationship between single measurable variables and product quality. The molten steel level in the mould has been shown to be one of the more important measurable variables [9]. To avoid potential defects, the fluctuation of this level must be reduced. As a result, most of the published papers related to the continuous casting control are focused on mould level control. An example can be seen in [10] where a PI controller with a variable gain and dither signal was implemented to control the mould level. The quality of steel level stabilization is shown to be considerably better when compared to the referential steel stream and using correction vibrating signal (dithering) is significantly better. Comparison between different control strategies including PI with high frequency dither, linear cascade controller and non-linear cascaded controller was conducted in [11]. Similarly to [10], the authors also used a high frequency dither signal to deal with the non-smooth nonlinearities of the signal. It was concluded that the nonlinear controller had a better performance as it required less control action but was able to dampen the mould level oscillations more efficiently.

1.1.2. Dynamic Bulging Disturbance

A common phenomenon that is being observed on the mould level is the bulging disturbance; bulging disturbance is mostly created by the supporting rollers that tend to push the liquid steel upward periodically [12]–[14]. Various control methodologies were proposed to compensate for this disturbance such as an adaptive sine estimator-based disturbance observer [15]. This observer was combined with a phase lead adaptive fuzzy controller. Both simulation and experimental results proved that the controller was able to reduce the bulging disturbance effect on the mould level. A similar attempt at suppressing the disturbance was done using a basic PI controller with an additional adaptive compensation that adapts the gain and prediction time to compensate for the disturbance [16]. Further attempts include a global observer that compensates for both bulging and the clogging/unclogging of the SEN [17]. In this case an online estimator tracks the effect of both external signals on the mould level. The control loop also uses the mould level, stopper position, and the flow rate as measurement signals. This allows for the fluctuations generated by the bulging to be drastically reduced. A similar approach is found in [18] where an observer is combined with a feed forward loop to reduce the mould level fluctuations.

It becomes clear that the majority of the papers discussed above use variables measured at specific points of the process rather than taking into account what is going inside the process itself, especially when considering the flow structure inside the mould. Although the mould level provides some information on what is going on inside the mould, it provides limited information on the flow structures of the mould. Therefore, it becomes logically to consider sensors that would allow us to see into the mould and extract more information on the flow structures.

1.2. Control Based on Multidimensional Measurement Data

There is growing interest towards utilizing multidimensional measurement data in industrial control. The advantage of these sensors is that they can provide information on what is happening inside the process itself, allowing us to control variables that were previously not attainable. As previously mentioned, control based on distributed sensing in the process of continuous casting is extremely limited, mainly these sensors are used for monitoring of the process rather implementation in a control loop [23]–[26]. In this section we will be concentrating on the general application of sensors based on multidimensional measurement data in controlling various processes and applications.

An example for control based on distributed parameter model is reported in [28]. The objective was to control the moisture content in a batch fluidised bed dryer. An electric capacitance tomography (ECT) was used to measure the moisture content. Also, in this case most aspects of the controlled plant behaviour were modelled using lumped parameter models based on mass and energy balances. This is then used to feed the permittivity model with the required moisture content variable. The permittivity model is a distributed parameter model that will calculate the permittivity distribution. The controller is then designed to keep the distributed permittivity around a desired shape using optimal control tools. This approach, where distributed parameter modelling is used just to describe those aspects of the plant behaviour whose distributed parameter modelling is essential while the rest is modelled using lumped parameters, seems to be generally promising as such models can be tractable analytically and suitable for use in the context of model-based control.

Furthermore, in [29] the author proposes a feedback control system based on Electrical Impedance Tomography (EIT) designed to regulate the concentration distribution of a substance in a fluid flowing through a pipe. The reconstruction algorithm allows for state predictions given by the evolution model, this is updated with the information provided by the measurements. A Linear Quadratic Gaussian (LQG) controller was applied using impedance tomographic measurements. The optimal values for the control input **u** are obtained by minimizing the quadratic cost function. Numerical simulations show that the control system was successful at obtaining the desired concentration on the output boundary. Furthermore, the state estimation and control strategies were shown to be relatively tolerant to misspecification of variables such as the velocity field which is important when it comes to more complex flows such as turbulent and multiphase flows.

1.3. Modelling in Continuous Casting

Computational Fluid Dynamics (CFD) methods such as Finite-difference modelling has been proven to produce reliable mathematical models that are able to

describe the interactions that occur in the continuous casting process. These models allow us to use model-based controllers such as Model Predictive Control (MPC) in order to achieve the necessary control objectives. However, due to the complexity of the whole process, it is not possible to model the entire process all together, instead the different phenomena are uncoupled, and assumptions are made to model them in isolation.

1.3.1.   Electromagnetic Actuators

Due to the importance of the fluid flow in the mould in improving steel cleanliness, it has become common practice to use electromagnetic actuators to somewhat control the flow in the mould. These actuators can be classified under the terms electromagnetic stirrers and electromagnetic brakes (EMBr) [30]–[32]. The concept behind electromagnetic stirrers is creating a rotating magnetic induction field to eventually create an electromagnetic force that is applied to the steel liquid. Electromagnetic brakes on the other hand generate a static magnetic field which creates Lorentz forces in order to brake the fluid motion. This phenomenon has been modelled frequently in various research; in [33] where a finite-volume model was implemented using theory of computational fluid dynamics and magneto-hydrodynamics. It was shown that both the magnetic induction intensity and the position of brake region affect the fluid flow in the mould. As the magnetic field is increased, both the recirculating flow velocity and the impingement intensity become weak. Similar results were achieved with an electromagnetic stirrer [34] showing that the stirrer position effects both the fluid flow and solidification process in the mould.

1.3.2.   Temperature Field

There has been significant interest in modelling the heat transfer and solidification process that occurs in continuous casting; models are used to predict to temperature distribution and the solidifying steel shell [30] in order to control the secondary cooling and achieve the optimum steel product. Typically, a mathematical heat transfer model is used to simulate the solidification process in the continuous caster using technical conditions from a steelmaking plant. In [36] the mathematical model formulation is based mainly on a two dimensional unsteady state heat transfer equation. Several boundary conditions are applied, and the initial condition for the steel casting temperature is measured in the tundish from the steel plant. The model was verified by comparing the calculated slab surface temperatures with the measured temperature results which resulted in a relative error of less than 1.95%. In the end, the model concluded that the casting speed, pattern of spray cooling zone, and slab size have the largest influence on the temperature field of the slab. By lessening the water flow rate and increasing the casting speed, the solidification process can be improved.

2. Doctoral Thesis Objectives

Based on the literature analysis, it becomes clear that the continuous casting process is a challenge when designing control systems due to the limitation of applying sensors. The existing control loops implemented in the continuous casting process are mainly limited to mould level control or temperature distribution control as these variables are currently readily available. However, many of the quality defects that occur in the end-product of the steel depend on the flow patterns in the liquid steel while in the mould. Issues such as slug entrapment, meniscus freezing, and other problems heavily determine the quality of the steel. Therefore, it is natural to look for solutions where we can try to 'see' inside the liquid steel before it is completely solidified.

The general objective of this doctoral thesis is to use two-dimensional flow monitoring in a control loop to improve the control of a continuous caster. Two such flow monitoring sensors will be considered: Ultrasound Doppler Velocimetry (UDV) and Contactless Inductive Flow Tomography (CIFT). UDV will be mainly used in designing both the process models and controller structures in this thesis. The main reason for this is that the experimental data were obtained using a small-scale continuous caster Mini-LIMMCAST where the UDV sensors were finalised at the beginning of the research described in this thesis. On the contrary, CIFT sensors were and still are under development to some extent. It can be expected that it will be possible to extend the techniques developed with UDV and transfer them into CIFT as both sensors can reconstruct the velocity profile in the mould.

The general objective of improving the control of a continuous caster can be naturally split into several sub-objectives. Firstly, a process model is necessary to design and test any at least somewhat advanced controller. Secondly, the general statement that the quality of the final product depends on the flow patterns in the mould is true, but by itself, it is not a sufficient basis for control. For this reason, the next objective must be to identify appropriate quantitative flow characteristics that could be used as controlled variables for efficient closed-loop control based on distributed data inside the mould.

Thirdly, the central objective is to develop the controllers that will use these quantitative characteristics as controlled variables while stopper rod position and magnetic field of the electromagnetic brake will be manipulated variables.

Last but not least, the thesis should discuss the possibility of transferring the developed methods and techniques to CIFT sensors. In the end, there should be a clear analysis on what are the best approaches regarding processing the sensor data, modelling the process, and designing model-based controllers for the continuous casting process.

The research done in this paper is a part of a European Training Network under the Marie Sklodowska-Curie Actions, under the name "Smart tomographic sensors for advanced industrial process control (TOMOCON)".

3. Model-Based Control Using System Identification

In this chapter we aim to find quantitative characteristics of the flow that can be used to optimise the flow in the mould. System identification will mainly be used to create the process models needed for the control loop. One of the main challenges in designing control loops for the continuous casting process is selecting the appropriate variables to achieve the optimum flow pattern needed in the mould. Now that two-dimensional flow monitorign allows us to view into the mould and have an understanding on the flow structures, we need to decide on what are the optimum flow characteristics that would yield higher quality steel, and how to control it with our actuators.

3.1.1. Process Modelling

A model is needed for both testing and designing the controller in the case of model-based control. System identification requires uniformly sampled time or frequency-domain data with the required inputs and outputs of the system. In our case our input will be the current to the EMBr, while the output if the angle of the exiting jet angle.

3.1.1.1.Linear Model

The first step will be to create a model for the process without any clogging present in the SEN. Process model estimation is used to create a transfer function describing the linear system dynamics. Through a process of trial and error where parameters including poles, zeros, and time delays are varied, the end result show that the relationship between EMBr current and jet angle can be described by a linear model in the form of a first order model [38], Where K_p represents the static gain and the T_{p1} represents the time constant.

$$G(s) = \frac{K_p}{1+sT_{p1}} \tag{3.1}$$

$$K_p = -0.0442 \tag{3.2}$$

$$T_{p1} = 1.44 \tag{3.3}$$
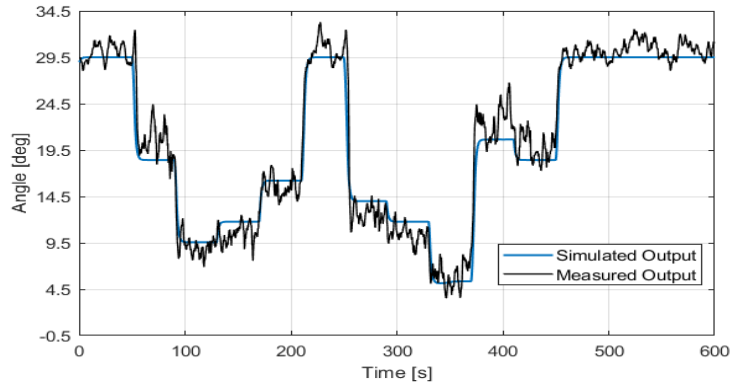
Figure 3.1. Comparison of simulated model output with measured output

12

Comparison of the first order model output with measurement (where the angle was calculated from the UDV data using the procedure described above) is shown in Figure 3.1. This figure gives the response to a series of random step changes of the EMBr current. It can be observed that there is a good fit between this first order model and measured data. Fast dynamics and relatively short time constant of model are due to the rapid responses of the velocity fields in the region of interest to the changes in the magnetic field produced by the brakes. It becomes clear that the relationship between brake current and jet angle can be described by a linear model in the form of the following first order model.

3.1.1.2.Non-Linear Model

As seen in Figure 3.2, it becomes clear that the linear model from the previous section is no longer sufficient to describe the dynamic response if clogging occurs as the fit percentage goes down to 65.99%. There are two fundamental differences; first, the oscillations of the angle are significantly higher with clogging.
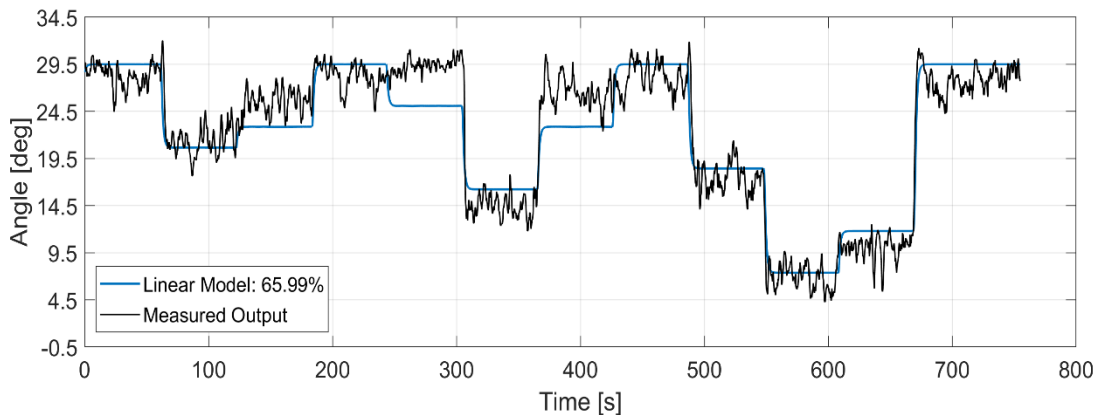
Figure 3.2. Comparison of Wiener model output with measured output

Therefore, non-linear models were investigated in order to improve the fit percentage. This led us to the Wiener model as we would like to keep the model as simple as possible while improving the fit percentage of the model. This approach is based on the concept of decoupling the linear behaviour from the non-linear behaviour. We will be utilizing the Wiener model for the second set of experiments; this set of experiments is used for modelling the dynamic response of the jet angle with clogging in the SEN as seen in Figure 3.3. The figure compares the response of the models to a series of random step changes to the EMBr current. The increased nonlinearity can be accounted for by adding a static nonlinearity to the linear model i.e. by using a Wiener model. The linear part of the Wiener model consists of a first order transfer function:

$$G(s) = \frac{K_p}{1+sT_{p1}} \tag{3.4}$$

$$K_p = 0.063 \tag{3.5}$$

$$T_{p1} = 1.7 \tag{3.6}$$

The output of the linear function is fed into a static nonlinear block in order to model the output nonlinearity. In this case, the Wiener model allows us to build on the linear transfer function and improve the fidelity of the model by adding a static non-linearity behaviour that has been introduced in the clogging state [40]. Both equations have similar absolute values for the time constant. The static nonlinear block in the Wiener model contains a piecewise linear function consisting of 2 breakpoints. Figure 3.3 shows that the added nonlinear function improves the performance of the model by 14.74%.
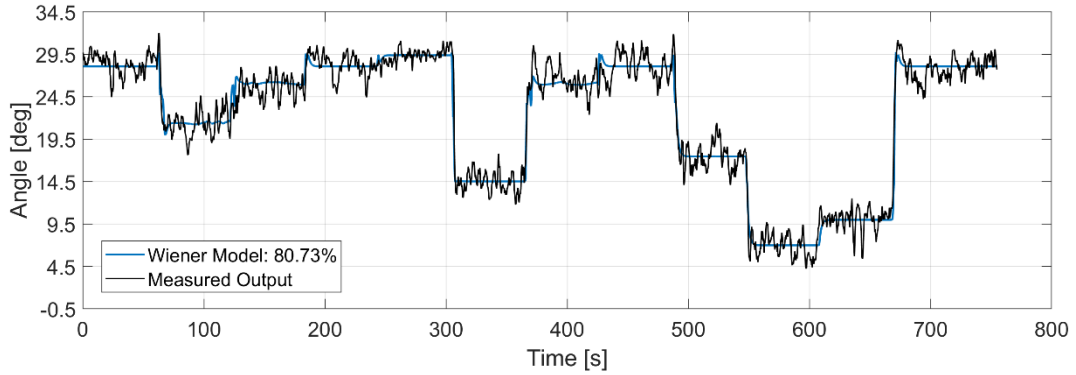
Figure 3.3. Comparison of Wiener model output with measured output

3.1.2. Controller Structure

3.1.2.1. Clogging Detection

The concept behind using the switched MPC is for the controller to modify its response depending on whether there is clogging or not in the SEN. SEN clogging changes the response of the jet angle to the changes to the current to EMBr as shown. The controller should be able to efficiently keep the angle of the jet between the optimum range in both cases of normal operation and during SEN clogging. In order to do so, the controller needs to detect if clogging has occurred during operation using information obtained from the angle of the jet. Figure 3.4 shows us the angle of the jet for two cases: Case 1 is taken from the first set of experiments where there was no SEN clogging during the measurements. Case 2 is taken from the second set of experiments where the SEN was partially clogged during the measurements. In both figures the EMBr is turned off. In the case of clogging, the angle of the jet oscillates more significantly than in the normal operation case. The signal contains higher frequencies. By taking advantage of this behaviour, we can detect the occurrence of clogging during operation by calculating the standard deviation of the signal along a moving window.

14
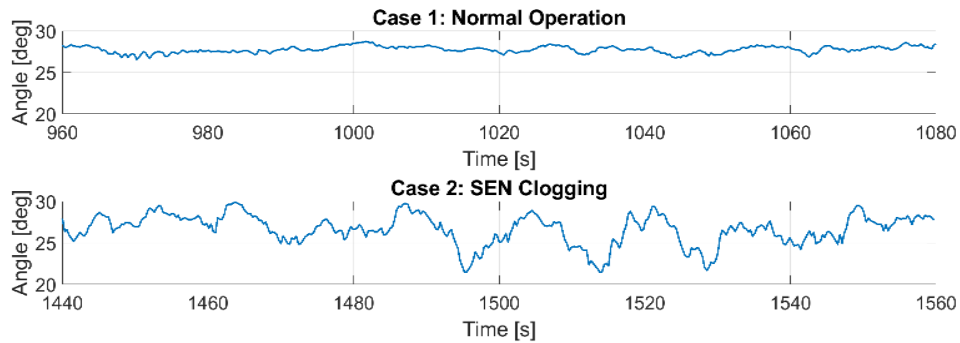
Figure 3.4. Comparison of jet angle with and without clogging

3.1.2.2. Model Predictive Control

Although Proportional-Integral-Derivative (PID) controllers are used in the majority of industrial applications, certain limitations make it unfavourable to apply PID controllers in specific processes. These include the difficulty of expanding the controller for MIMO processes due to interactions between loops. Also, PID controllers themselves are unable to incorporate constraints on manipulated variables and controlled variables. A possible solution for these issues is the use of Model Predictive Control (MPC). An additional advantage of MPC is their ability to predict the future effect of control actions and optimize them in order to achieve the desired behaviour.

3.1.2.3. Switched MPC

Following the formulation of the MPC, the next step will be to design the Switched MPC in order to deal with the two scenarios of clogged and unclogged states. Switched MPC has been successfully implemented in processes that exhibit multiple modes [41], [42]. The main concept is that the controller is able to transition between multiple MPC controllers in real time based on the operating conditions. This is usually done by designing each controller based on a specific region of the operating space. By using a switching signal, the current operating region is detected and based on this the appropriate active controller is selected.

3.1.3. Testing and Results

Two sets of simulations were implemented; the first simulation included the MPC based on the linear model. In this simulation we are performing set point tracking in the case where there is no clogging and analysing the controller's response to various changes to the set point (see Figure 3.5 and 3.6). The controller is able to successfully track the set point with an average settling time of t=5s. In the end, the controller performance is shown to be sufficient for controlling the exiting jet angle. The response of the controller is fast enough for the dynamics of the system. In the second simulation we are testing the switched

MPC and simulating the clogging affect to see how the controller will respond. Figure 3.7 shows that from t=0s to t=75s the model for normal operation is used, at t=75s the model is switched to the clogged model to simulate clogging in steel casters. We can see that even without the clogging being detected by the controller, the MPC is able to perform the needed action to bring the angle of the jet to the required set point. At t=100s we simulate the clogging being detected and the switching to the second MPC that is designed for the clogging model. It is clear that the transition from the first MPC to the second occurs smoothly with the set point being tracked efficiently. At t=150s the controller is also able to effectively track the set point with the presence of clogging in the process.
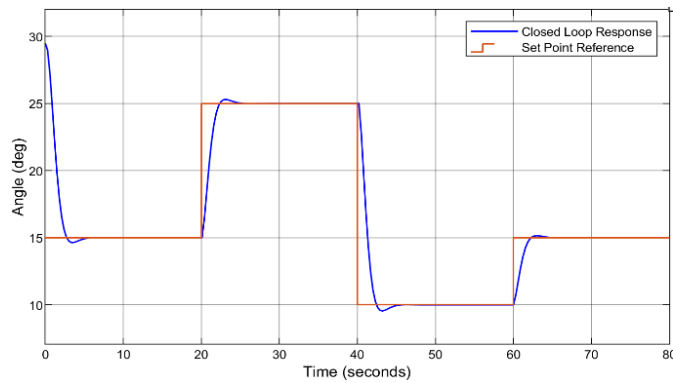
Figure 3.5. Closed loop response for set point tracking
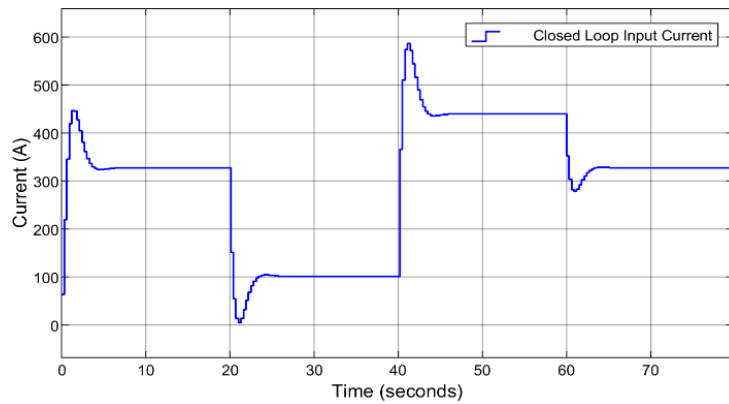
Figure 3.6. Input current for set point tracking

16
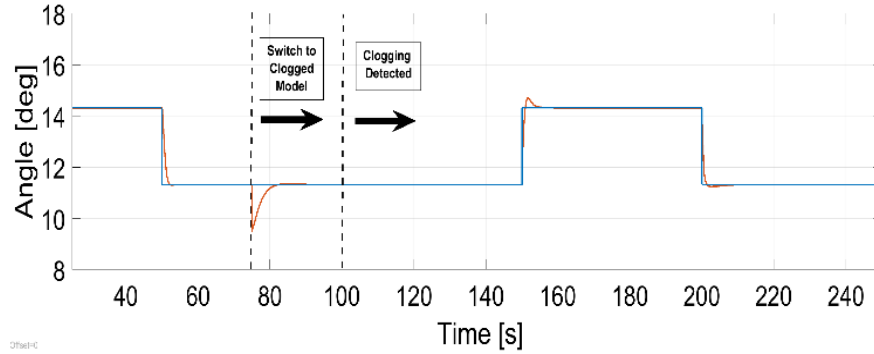
Figure 3.7. Comparison of model output with set-point reference
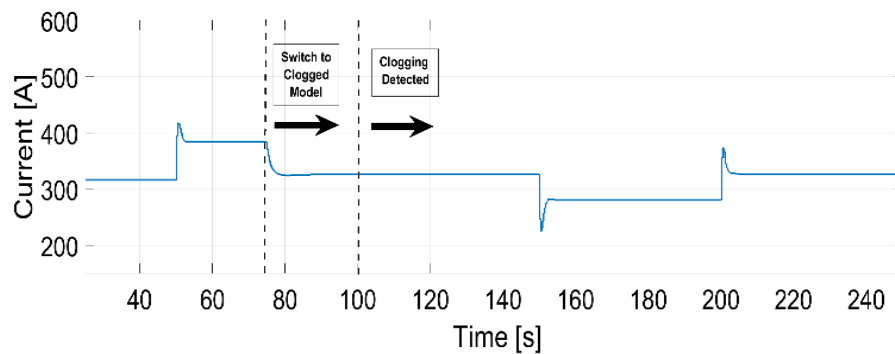
Figure 3.8. Input current for set-point tracking

3.2.   Meniscus Velocity

In this section, we move away from the exiting jet to the meniscus velocity as our controlled variable. Meniscus velocity in continuous casting is critical in determining the quality of the steel, it needs to be kept between a specific range; too high velocities create excessive turbulences that can increase the potential of slug entrapment. On the other hand, too low meniscus velocities result in excessive cooling which can cause various surface defects as well [7]. Due to the complex nature of the various interacting phenomena in the process, designing model-based controllers proves to be a challenge. Therefore, a NARX neural network model is trained to describe the complex relationship between the applied current to an EMBr and the measured meniscus velocity. Adaptive Model Predictive Control (MPC) is used to deal with the non-linearity of the model by adapting the prediction model to the different operating conditions. The results in this section were published in [43].

3.2.1.   NARX Neural Network Model

Using experimental data, a dynamic neural network with feedback connections was designed using a nonlinear autoregressive model with exogenous inputs (NARX). The

NARX model is based on the linear ARX model but instead of using the weighted sum of its regressors to predict the current output, it uses a nonlinear mapping function *f*. In our case the nonlinearity estimator will be done using the neural network. The neural network time series toolbox in MATLAB was used to design the model.

The NARX network consists of a two-layered feedforward network. A sigmoid function is used in the hidden layer, while a linear transfer function is used in the output layer. The tapped delay line allows for previous input and output values to be stored. The input x(t) represents the current going to the EMBr, while the output y(t) represents the meniscus velocity. It is clear that a feedback connection is needed for the network to take in previous values of the meniscus velocity in order to create the dynamic model. In our case 10 hidden neurons were used, with the number of delays of 2.

3.2.2. Adaptive MPC

The main objective of the control loop is to maintain the meniscus velocity within the optimum range and to reject disturbances during the process. Besides minimum and maximum limits related to the optimum range of the meniscus velocity, there is also the maximum limit on the current of the EMBr. As it is evident from the previous section, the controlled plant is not only nonlinear but there are other issues as well. This nonlinearity is not well amenable to analytic description and it may be time varying. This would complicate the use of nonlinear MPC. We also regarded it as desirable to keep the beneficial features of MPC based on linear models and quadratic programming. For all of these reasons our approach of choice is to implement adaptive MPC where online model estimation is used to update the internal plant model in order to achieve a reasonable level of control performance with this nonlinear plant. This adaptive MPC is based on continuously updated linearized model. For this purpose, NARX Neural network is linearized and converted to the discrete time state space. A recursive polynomial model estimator is used for the online model estimation. This is used to update the internal model of the MPC by linearizing the NARX model

3.2.3. Testing and Results

The experiments concentrate on disturbance rejection (see Figure 3.9 and 3.10) which is the main objective of this study. One of the main disturbances in the continuous casting process is the changing of the casting speed. The casting speed is changed sporadically throughout the process; it would be valuable to see if an automatic control loop can keep the meniscus velocity in the optimum range and reject the effect that might occur from changing the casting speed. The disturbance from changing the casting speed will be applied at the output of the model; increasing the casting speed results in an increase in the meniscus velocity.
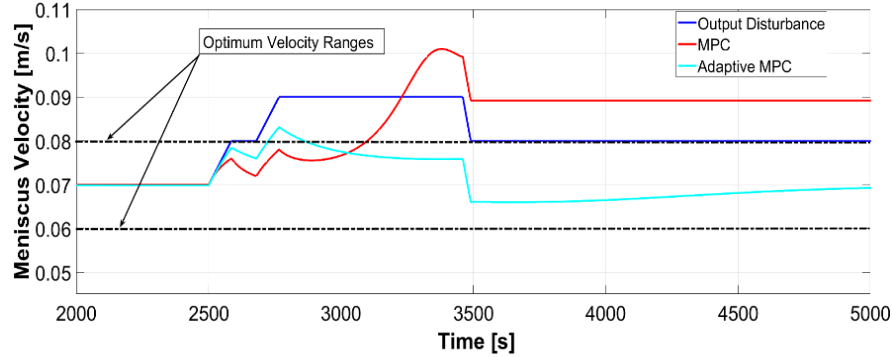
Figure 3.9. Closed loop response for disturbance rejection
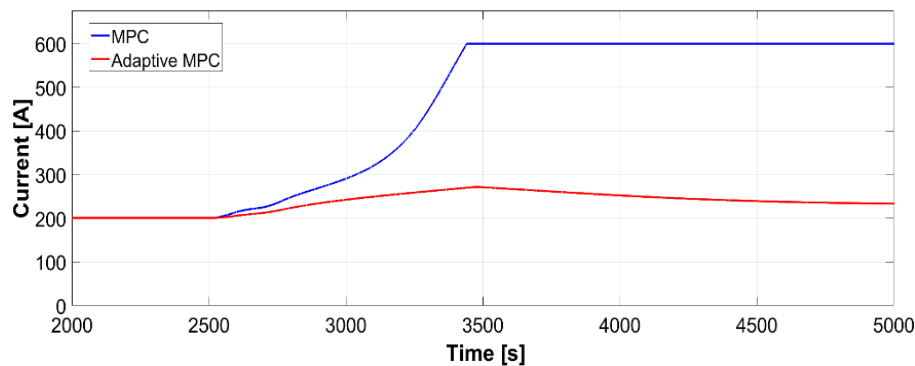
Figure 3.10. Input current for disturbance rejection

In Figure 3.10 we compare the performance of a conventional MPC with the adaptive MPC. The disturbance on the output was taken from [7]. Both the MPC and adaptive MPC respond to this disturbance in order to keep the meniscus velocity between the optimum ranges. In the case of the adaptive MPC, the velocity slightly goes beyond the range at T=2725s but it is then brought back to the optimum range at T=2860s. On the other hand, the conventional MPC goes beyond the optimum range at T=3100s and is unable to bring the velocity back to the optimum range for the remainder of the experiment. This is due to the saturation that occurs in the manipulated variable as shown in Figure 3.10. We can clearly see here that the adaptive MPC outperforms the conventional MPC due to its ability to deal with the nonlinearity of the system, especially at the higher current ranges of the EMBr where this non-linearity is even more present.

3.3.   MIMO Control Loop

Previous experiments have included only the EMBr as the manipulated variable; the next step will be to extend the control loop to multiple input-multiple output by using both EMBr and stopper rod to control the flow in the mould. In this section, we are moving away from the meniscus velocity and concentrating once again on the exiting jet. Although section 3.2 shows that the meniscus velocity can be controlled and kept within optimum

ranges using the EMBr, there is a more direct effect on the exiting jet from our actuators. For this reason, we are basing our MIMO controller on features related to the exiting jet including the jet impingement point and the jet velocity. The results in this section were published in [44].

3.3.1. Extracting Controllable Features

For the case of the continuous caster, we need to determine the specific features of the flow in the mould that can help improve the quality of the steel, and at the same time can be controlled using our manipulated variables. The two features chosen in this paper for control are the jet impingement point on the narrow wall, and the velocity of the exiting jet.

3.3.1.1. Jet Impingement

The jet impingement point defines how deep or shallow the jet impinges into the mould. The optimum case is to keep the jet as close to the horizontal baseline as possible to ensure a shallow impingement. As shown in Figure 3.11, this feature can be quantified by calculating the mean value of the velocity field between UDV sensors 5 to 7 (−0.07 m to −0.09 m from the surface level). If the value increases, it is more likely that the exiting jet is oscillating in this region. The value of the mean velocity will be used as the controlled variable.

(**a**)   (**b**)
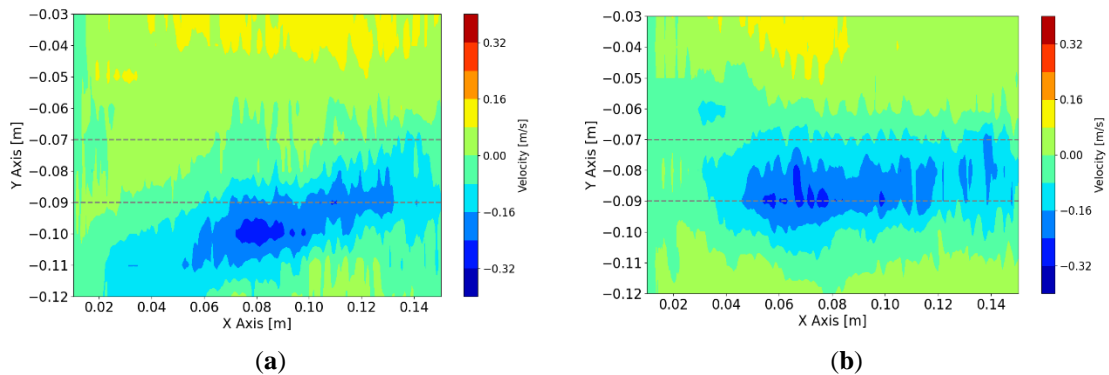
Figure 3.11. Reconstruction of velocity profile with identified shallow region to quantify jet impingement (a) t = 300 s, (b) t = 800 s.

3.3.1.2. Jet Velocity

The idea of using the velocity of the exiting jet is based on section 3.1 where a straight line is used to represent the exiting jet. In this section, we will be extending this concept to include a more realistic shape of the jet, which has sometimes a more 'banana' like shape. In order to model this adequately, a third-degree polynomial is used to fit the shape of the jet during each captured frame as shown in Figure 3.12. It is clear that the

polynomial can track the movement and shape of the jet efficiently. The controlled variable is the overall velocity of the jet and is the mean of the velocities along the polynomial.

(a)   (b)
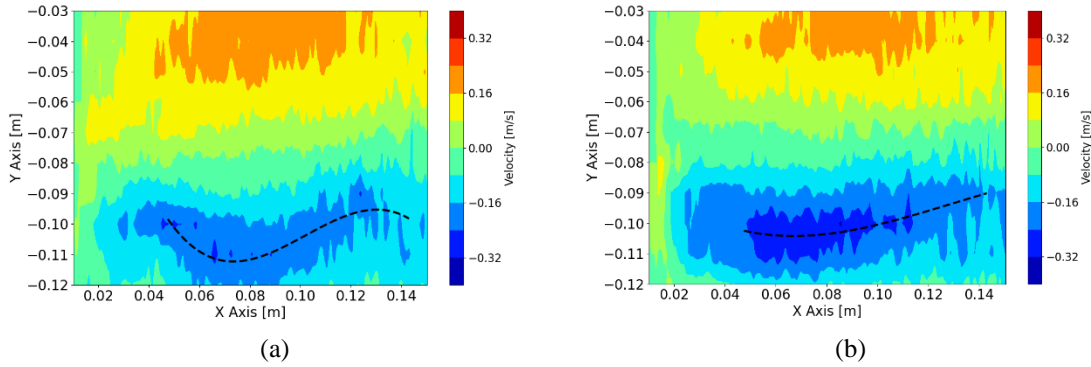
Figure 3.12. Reconstruction of velocity profile with tracking of jet shape to quantify jet velocity, (a) t = 500 s, (b) t = 600 s

3.3.2.   State Space Estimation

A black-box model is created based on both extracted features from the UDV measurements and applying system identification to determine the dynamic relationship between the inputs and outputs. A 2-input, 2-output model is created where the inputs are the current of electromagnetic brake and the stopper rod position, while the outputs are the jet impingement point and the jet velocity. The current of the brake was varied from 0 to 600 A, while the lifting of the stopper rod position was between 5–10 mm. State space estimation using subspace was used in this section. The output of the state space model was compared with the measurement output in Figure 3.13 and 3.14. The model is able to track the deterministic part of the signal which is the dynamic response due to the changes to the manipulated variables.
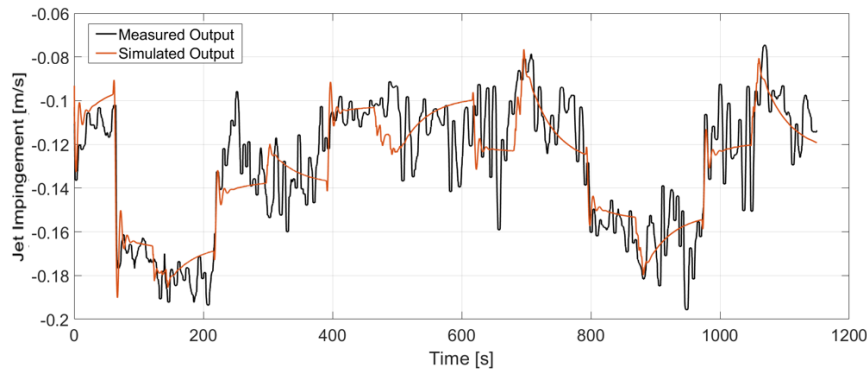
Figure 3.13. Comparison of the output of model with the measured output for jet impingement.
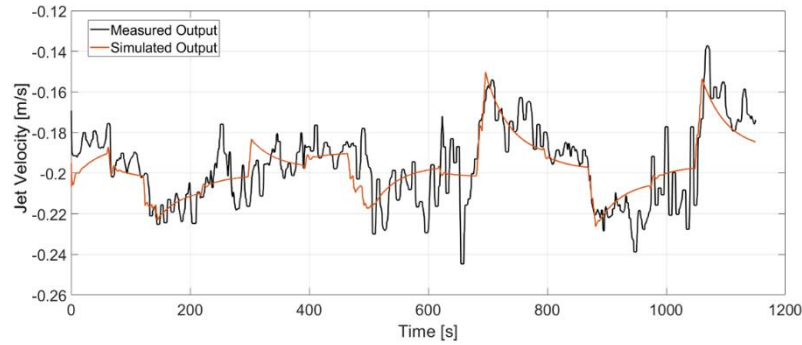
Figure 3.14. Comparison of the output of model with the measured output for jet velocity.

3.3.3. MPC Based on MIMO Model

As mentioned before, MPC algorithms can easily be expanded for multivariable control problems. The cost function J can be expanded to include multiple controlled and manipulated variables. The main control objectives for the experiments conducted in this section are to achieve a shallow jet impingement and maintain the jet velocity within an optimum range.

3.3.4. Testing and Results

In Figure 3.15 and 3.16 the dynamic response of the system to the changes in the set-points is presented. A stochastic signal is superimposed at the output to emulate the effect of turbulence. At t = 100 s a negative step input is applied to both set-points, while at t = 250 s a positive step input is applied. The figures show that the controller can track both set-points in the positive and negative step changes. Both dynamic responses have a settling time of ~20 s, although the jet velocity overshoots the set-point before settling down. Furthermore, Figure 3.17 and 3.18 show the manipulated variables during the experiments. The controller can achieve the control objectives without exceeding the constraints on the manipulated variables.
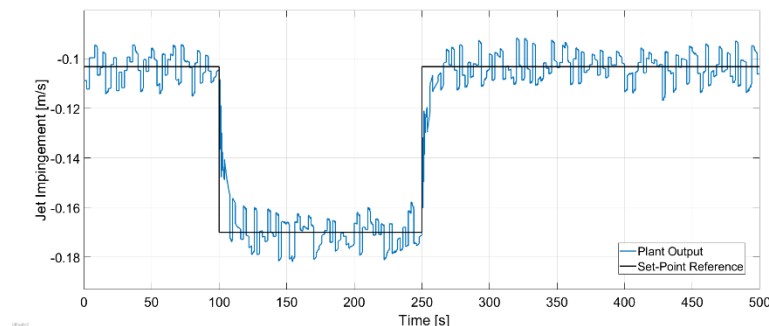
Figure 3.15. Closed loop response of jet impingement for set-point tracking.
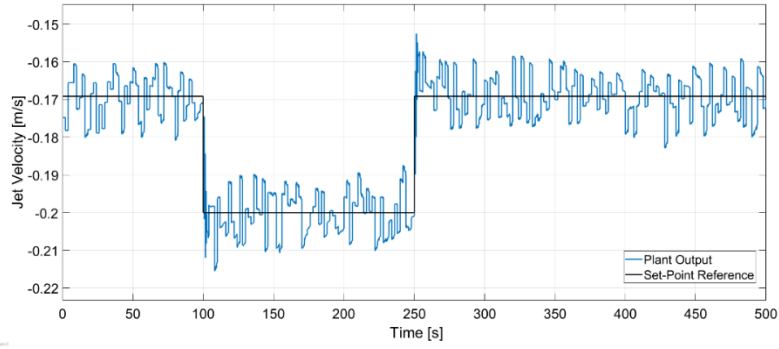
Figure 3.16. Closed loop response of jet velocity for set-point tracking.
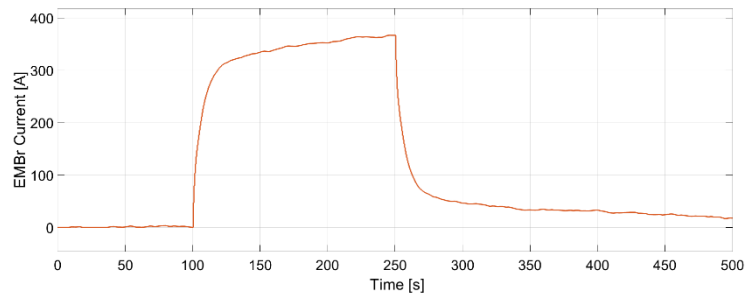
Figure 3.17. Changes of electromagnetic brake current.
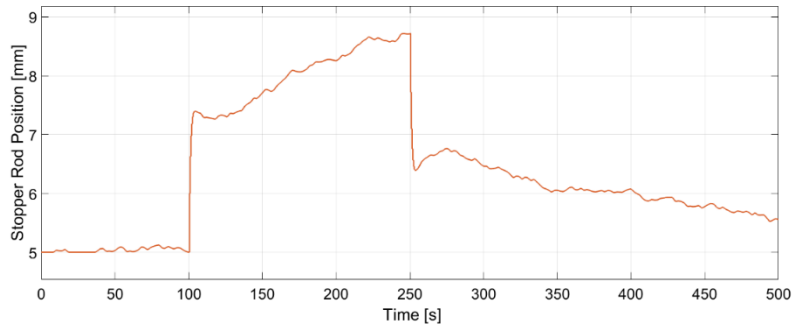
Figure 3.18. Changes of the stopper rod position generated by the controller to track the jet velocity.

4. Control Loop Structure Based on CIFT

CIFT is a tomographic sensor that is able to measure the multi-dimensional velocity fields of conductive fluids; this is done by measuring the perturbations of an applied magnetic field caused by the flow of the conductive fluid. Similarly, to UDV, this sensor can be applied to the mould of the continuous caster in order to provide multidimensional data on the velocity fields. While UDV is able to obtain velocity component in one direction of the ultrasound beam, CIFT is able to measure the three-dimensional velocity fields. The main concept of the CIFT technique relies on the flow of the conductive liquid going through a magnetic field created by the CIFT transmitter sensors. This creates electrical currents in the mould which results in an induced magnetic field. The induced magnetic field is measured by the receiver sensors and is used to reconstruct the velocity field in the mould. Figure 4.1 shows the reconstructed velocity profile from an experiment conducted on the Mini-LIMMCAST setup. The figure shows that we are able to reconstruct both sides of the mould, in this case we can see a clear double roll flow in the mould.
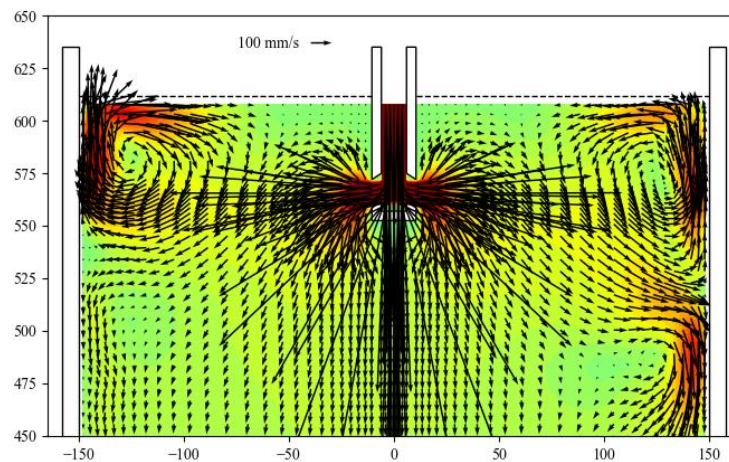
Figure 4.1. Reconstructed velocity profile from CIFT showing a double roll flow in the mould

In this chapter, we will extend the techniques used for UDV measurements to CIFT measurements for the purpose of control. The exiting jet angle will be obtained from the 3-D velocity fields from the CIFT data. The feasibility of using CIFT in a control loop similarly to UDV will be analysed. In the case of UDV measurements, we concentrated on the mid-region between the SEN and the narrow face wall. Velocities near the narrow face wall were avoided due to the turbulence affecting the accuracy near the wall. In the case of CIFT, we instead concentrate on the velocities near the narrow phase wall because it is more accurate than the velocities in the mid-region. This is due to the fact that velocities closer to the receiver sensors have a higher accuracy compared to the velocities in the mid-

region. By concentrating on the narrow face wall, we are able to identify the impingement point of the jet and correlate this with the jet angle.
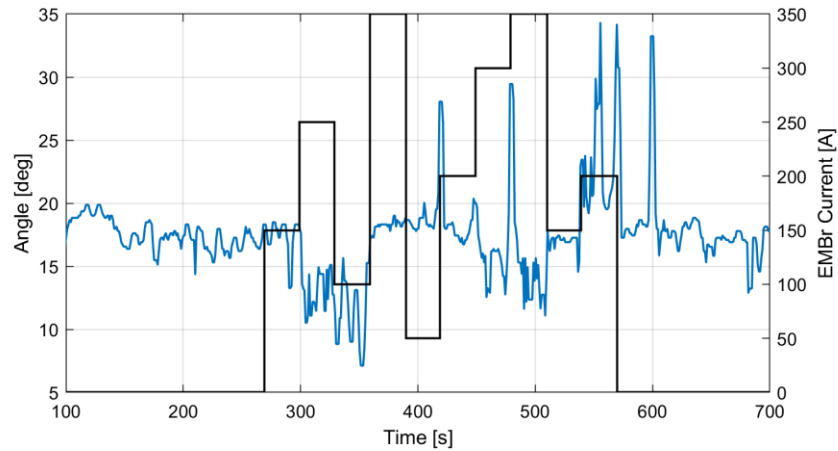
Figure 4.2. Response of jet angle to current changes to the EMBr on left half of mould

Figure 4.2 depicts the angle of the jet in response to random changes to the EMBr current. Random current steps are applied to the EMBr to record the full dynamics of the process, while the CIFT sensors measure the induced magnetic field. This induced magnetic field is used to reconstruct the velocity fields, where the angle of the jet is obtained from the impingement point on the narrow face wall. The figure shows that it is difficult to conclude a clear relationship between the angle of the jet and the EMBr current. It is expected that the CIFT sensors would not produce equally clear results as UDV because UDV relies on the direct measurements of the ultrasound beams, while CIFT requires an added step of the linear inverse problem to reconstruct. Although the potential of using CIFT for control of the continuous caster is there, the accuracy of the reconstruction algorithm requires further improvement due to the effect of the EMBr applied magnetic field. The main challenge faced by CIFT in the process of the continuous caster is the applied magnetic field from the EMBr. The EMBr requires large ferromagnetic pole shoes in order to amplify the magnetic field of the brake, which has an effect on the excitation field. Therefore, in order to use the EMBr in a control loop, the magnetic field of the EMBr has to be readjusted accordingly.

5. Summary and Conclusion

The general objective of this doctoral thesis was to use two-dimensional flow monitoring sensors in a control loop to improve the control of a continuous caster. This objective was motivated by the fact that many of the quality issues occurring in the end product of the continuous casting process are related to the flow patterns in the mould. By utilizing these sensors, we can obtain information on the flow structure in the mould in a non-invasive manner. This thesis mainly used ultrasound Doppler Velocimetry (UDV) as the flow monitoring sensor.

In Chapter 3 we aimed to create a process model using system identification using data coming from UDV. The Mini-LIMMCAST setup allowed us to obtain experimental data from the sensors and use them to create the models needed for control design and model-based control. However, multivariable measurements from UDV sensors could not be used directly for identification because they cannot be considered controlled variables for which set points can be specified. It was necessary to find appropriate quantitative flow characteristics that could be used as controlled variables for efficient closed-loop control.

At first, we considered EMBr as a manipulated variable, which means there should be just one controlled variable. The exiting jet angle was proposed as a first quantitative characteristic that could be used as a single controlled variable. Experimental data from the Mini-LIMMCAST setup was used to create a transfer function describing the relationship between the EMBr and the angle of the jet. An MPC was designed to control this angle and keep it within optimum ranges under disturbance. This idea was extended in section 3.1.2. by using experimental data from a clogged SEN to design an algorithm that would detect SEN clogging by analyzing the oscillations of the jet angle. This information was then used to create a switched MPC that could control the system whether there was clogging or not in the SEN. An alternative characteristic was investigated in section 3.2, where meniscus velocity was used as a variable controllable by the EMBr. In this case, it was found by analyzing the experimental data that the dynamic relationship between EMBr and meniscus velocity is nonlinear. For this reason, a NARX neural network had to be employed to describe the relationship, and adaptive MPC had to be developed instead of standard MPC based on one fixed model. It has turned out that this adaptive MPC can cope with the system's nonlinearities successfully without violating the process constraints.

Lastly, in section 3.3, the control was extended to the multivariable case by introducing the stopper rod position as another manipulated variable besides the EMBr. The investigation has shown that jet impingement point and jet velocity are the most suitable controllable flow characteristics in the case of this two-input, two-output control configuration. Similarly, as in the case of single-input, single-output control configuration, system identification was used to obtain the control-oriented model. A fourth-order discrete state-space model described the deterministic component of the process response with

sufficient precision. However, there was also a significant unmodelled stochastic component resulting from the turbulent flow. Despite this, the model was precise enough to be used as a part of the model-based predictive controller, which could track both set-points without exceeding any constraints. In this way, optimal flow structures in the mould could be achieved.

In the end, it can be stated that several characteristics can be extracted from the UDV measured velocity profiles in the region surrounding the SEN in the mould. These characteristics can be used by model-based controllers in single-variable or two-variable configurations to adjust the flow structure in the mould according to the specified set points. The techniques used for control loop design can be extended to other sensors based on multidimensional data if similar information on the velocity fields of the mould is obtained. In Chapter 6, we attempted to extend these techniques to CIFT, where we used the velocity profile to obtain the exiting jet angle. Although CIFT is able to reconstruct the flow structures in the mould successfully, an issue occurs when introducing changes to the EMBr current. The main reason for this is the effect of the EMBr magnetic field and especially of the magnetic hysteresis associated with the ferromagnetic parts of the EMBr on CIFT measurements. It is possible to build a model of these hysteretic effects and compensate for them. CIFT can then be utilized in a control loop similarly to UDV. However, correct compensation for continuous-valued EMBr current (and not only for one or several discrete values of this current) remains still an open research problem.

Despite these remaining issues, it can be stated in conclusion that it has been shown that two-dimensional flow monitoring can be utilized in a control loop to control the flow structure in the mould of a continuous caster. The first objective of creating a process model was achieved mainly through system identification. Furthermore, by quantifying flow characteristics using the exiting jet, meniscus velocity, jet impingement point, and jet velocity, we could achieve our next objective of identifying characteristics that can be utilized as controlled variables for optimizing the flow in the mould. Lastly, through designing and testing various control strategies, we can achieve our third major objective of developing controllers using the necessary quantitative flow characteristics.

An interesting objective for future work would be to introduce more complex actuators to the process to achieve even better control over the flow in the mould. An example of this can be an electromagnetic stirrer that creates a rotating magnetic induction field and corresponding electromagnetic force applied to the steel liquid. The combined actuators can potentially allow us to optimize the flow patterns on both sides of the mould.

6. References

[1]   S. Louhenkilpi, "Chapter 1.8 - Continuous Casting of Steel," in *Treatise on Process Metallurgy*, S. Seetharaman, Ed. Boston: Elsevier, 2014, pp. 373–434. doi: 10.1016/B978-0-08-096988-6.00007-9.

[2]   I. K. Craig, F. R. Camisani-Calzolari, and P. C. Pistorius, "A contemplative stance on the automation of continuous casting in steel processing," *Control Engineering Practice*, p. 8, 2001.

[3]   L. Zhang, S. Yang, K. Cai, J. Li, X. Wan, and B. G. Thomas, "Investigation of Fluid Flow and Steel Cleanliness in the Continuous Casting Strand," *Metallurgical and Materials Transactions B*, vol. 38, no. 1, pp. 63–83, Apr. 2007, doi: 10.1007/s11663-006-9007-0.

[4]   B. G. Thomas, "Review on Modeling and Simulation of Continuous Casting," *steel research international*, vol. 89, no. 1, p. 1700312, Jan. 2018, doi: 10.1002/srin.201700312.

[5]   B. G. Thomas, "Modeling of the continuous casting of steel—past, present, and future," *Metall Mater Trans B*, vol. 33, no. 6, pp. 795–812, Dec. 2002, doi: 10.1007/s11663-002-0063-9.

[6]   B. G. Thomas, "On-line Detection of Quality Problems in Continuous Casting of Steel," p. 16, 2003.

[7]   R. Liu, B. G. Thomas, J. Sengupta, S. D. Chung, and M. Trinh, "Measurements of Molten Steel Surface Velocity and Effect of Stopper-rod Movement on Transient Multiphase Fluid Flow in Continuous Casting," *ISIJ Int.*, vol. 54, no. 10, pp. 2314–2323, Oct. 2014, doi: 10.2355/isijinternational.54.2314.

[8]   K. Cukierski and B. G. Thomas, "Flow Control with Local Electromagnetic Braking in Continuous Casting of Steel Slabs," *Metallurgical and Materials Transactions B*, vol. 39, no. 1, pp. 94–107, Feb. 2008, doi: 10.1007/s11663-007-9109-3.

[9]   H. Kitada, O. Kondo, H. Kusachi, and K. Sasame, "H Control of Molten Steel Level in Continuous Caster," *IEEE TRANSACTIONS ON CONTROL SYSTEMS TECHNOLOGY*, vol. 6, no. 2, p. 8, 1998.

[10]   L. Smutný, R. Farana, A. Víteček, and D. Kačmář, "MOULD LEVEL CONTROL FOR THE CONTINUOUS STEEL CASTING," *IFAC Proceedings Volumes*, vol. 38, no. 1, pp. 163–168, 2005, doi: 10.3182/20050703-6-CZ-1902.01706.

[11]   Graebe, Goodwin, West, and Stepien, "An application of advanced control to steel casting," 1994, pp. 1533–1538 vol.3. doi: 10.1109/CCA.1994.381488.

[12]   C. Furtmüller, P. Colaneri, and L. del Re, "Adaptive robust stabilization of continuous casting," *Automatica*, vol. 48, no. 1, pp. 225–232, Jan. 2012, doi: 10.1016/j.automatica.2011.09.049.

[13]   J. S. Ha, J. R. Cho, B. Y. Lee, and M. Y. Ha, "Numerical analysis of secondary cooling and bulging in the continuous casting of slabs," *Journal of Materials Processing Technology*, vol. 113, no. 1, pp. 257–261, Jun. 2001, doi: 10.1016/S0924-0136(01)00654-9.

[14]   R. Guan, C. Ji, C. Wu, and M. Zhu, "Numerical modelling of fluid flow and macrosegregation in a continuous casting slab with asymmetrical bulging and mechanical reduction," *International Journal of Heat and Mass Transfer*, vol. 141, pp. 503–516, Oct. 2019, doi: 10.1016/j.ijheatmasstransfer.2019.06.079.

[15]   M. Kim, S. Moon, C. Na, D. Lee, Y. Kueon, and J. S. Lee, "Control of mold level in continuous casting based on a disturbance observer," *Journal of Process Control*, vol. 21, no. 7, pp. 1022–1029, Aug. 2011, doi: 10.1016/j.jprocont.2011.06.003.

[16]   C. Furtmueller and L. del Re, "Disturbance suppression for an industrial level control system with uncertain input delay and uncertain gain," in *2006 IEEE Conference on Computer Aided Control System Design, 2006 IEEE International Conference on Control Applications, 2006 IEEE International Symposium on Intelligent Control*, Oct. 2006, pp. 3206–3211. doi: 10.1109/CACSD-CCA-ISIC.2006.4777151.

[17]   K. Jabri, E. Godoy, D. Dumur, A. Mouchette, and B. Bèle, "Cancellation of bulging effect on mould level in continuous casting: Experimental validation," *Journal of Process Control*, vol. 21, no. 2, pp. 271–278, Feb. 2011, doi: 10.1016/j.jprocont.2010.10.020.

[18]   K. Jabri, B. Bele, A. Mouchette, D. Dumur, and E. Godoy, "Suppression of periodic disturbances in the continuous casting process," in *2008 IEEE International Conference on Control Applications*, Sep. 2008, pp. 91–96. doi: 10.1109/CCA.2008.4629617.

[19]   J. Zhang, D. Chen, S. Wang, and M. Long, "Compensation Control Model of Superheat and Cooling Water Temperature for Secondary Cooling of Continuous Casting," *steel research international*, vol. 82, no. 3, pp. 213–221, 2011, doi: 10.1002/srin.201000148.

[20]   J. Ma, Z. Xie, and G. Jia, "Applying of Real-time Heat Transfer and Solidification Model on the Dynamic Control System of Billet Continuous Casting," *ISIJ Int.*, vol. 48, no. 12, pp. 1722–1727, 2008, doi: 10.2355/isijinternational.48.1722.

[21]   Y. Wang, D. Li, Y. Peng, and L. Zhu, "Computational modeling and control system of continuous casting process," *Int J Adv Manuf Technol*, vol. 33, no. 1–2, pp. 1–6, May 2007, doi: 10.1007/s00170-006-0451-4.

[22]   C. Belavý, G. Hulkó, L. Bartalský, and M. Kubiš, "Robust Control of Temperature Fields in Steel Casting Mould as Distributed Parameter Systems," *IFAC-PapersOnLine*, vol. 48, no. 14, pp. 408–413, Jan. 2015, doi: 10.1016/j.ifacol.2015.09.491.

[23]   D. Xie, Z. Huang, H. Ji, and H. Li, "An Online Flow Pattern Identification System for Gas amp;#8211;Oil Two-Phase Flow Using Electrical Capacitance Tomography," *IEEE Transactions on Instrumentation and Measurement*, vol. 55, no. 5, pp. 1833–1838, Oct. 2006, doi: 10.1109/TIM.2006.881558.

[24]   T. Dyakowski, L. F. C. Jeanmeure, and A. J. Jaworski, "Applications of electrical tomography for gas–solids and liquid–solids flows — a review," *Powder Technology*, vol. 112, no. 3, pp. 174–192, Oct. 2000, doi: 10.1016/S0032-5910(00)00292-8.

[25]   D. Zhao *et al.*, "The control and maintenance of desired flow patterns in bends of different orientations," *Flow Measurement and Instrumentation*, vol. 53, pp. 230–242, Mar. 2017, doi: 10.1016/j.flowmeasinst.2016.09.003.

[26]   Y. Zhang and X. Ai, "The Identification of Two-Phase Flow Regimes Using HMM Model Based on ERT System and PCA Feature Extraction," in *2014 Fifth International Conference on Intelligent Systems Design and Engineering Applications*, Jun. 2014, pp. 1053–1055. doi: 10.1109/ISDEA.2014.232.

[27]   P. D. Christofides, "Control of nonlinear distributed process systems: Recent developments and challenges," *AIChE Journal*, vol. 47, no. 3, pp. 514–518, 2001, doi: 10.1002/aic.690470302.

[28]   J. A. Villegas, S. R. Duncan, H. G. Wang, W. Q. Yang, and R. S. Raghavan, "Distributed parameter control of a batch fluidised bed dryer," *Control Engineering Practice*, vol. 17, no. 9, pp. 1096–1106, Sep. 2009, doi: 10.1016/j.conengprac.2009.04.012.

[29]   A. Seppänen, "State Estimation in Process Tomography PhD thesis."

[30]   B. G. Thomas and S. M. Cho, "Overview of Electromagnetic Forces to Control Flow During Continuous Casting of Steel," *IOP Conf. Ser.: Mater. Sci. Eng.*, vol. 424, p. 012027, Oct. 2018, doi: 10.1088/1757-899X/424/1/012027.

[31]   B. G. Thomas and R. Chaudhary, "State of the Art in Electromagnetic Flow Control in Continuous Casting of Steel Slabs: Modeling and Plant Validation," p. 6, 2009.

[32]   L. B. Trindade, J. E. A. Nadalon, A. C. Contini, and R. C. Barroso, "Modeling of Solidification in Continuous Casting Round Billet with Mold Electromagnetic Stirring (M-EMS)," *steel research international*, vol. 88, no. 4, p. 1600319, 2017, doi: 10.1002/srin.201600319.

[33]   Y. Haiqi, W. Baofeng, L. Huiqin, and L. Jianchao, "Influence of electromagnetic brake on flow field of liquid steel in the slab continuous casting mold," *Journal of Materials Processing Technology*, vol. 202, no. 1–3, pp. 179–187, Jun. 2008, doi: 10.1016/j.jmatprotec.2007.08.054.

[34]   A. Maurya and P. K. Jha, "Influence of electromagnetic stirrer position on fluid flow and solidification in continuous casting mold," *Applied Mathematical Modelling*, vol. 48, pp. 736–748, Aug. 2017, doi: 10.1016/j.apm.2017.02.029.

[35]   K. Dekemele, C.-M. Ionescu, M. De Doncker, and R. De Keyser, "Closed loop control of an electromagnetic stirrer in the continuous casting process," Jun. 2016, pp. 61–66. doi: 10.1109/ECC.2016.7810264.

[36]   H. Wang, G. Li, Y. Lei, Y. Zhao, Q. Dai, and J. Wang, "Mathematical Heat Transfer Model Research for the Improvement of Continuous Casting Slab Temperature," *ISIJ Int.*, vol. 45, no. 9, pp. 1291–1296, 2005, doi: 10.2355/isijinternational.45.1291.

[37]   R. Isermann and M. Münchhof, "Correlation Analysis with Continuous Time Models," in *Identification of Dynamic Systems: An Introduction with Applications*, R. Isermann and M. Münchhof, Eds. Berlin, Heidelberg: Springer, 2011, pp. 149–178. doi: 10.1007/978-3-540-78879-9_6.

[38]   S. Abouelazayem, I. Glavinić, T. Wondrak, and J. Hlava, "Control of Jet Flow Angle in Continuous Casting Process using an Electromagnetic Brake," *IFAC-PapersOnLine*, vol. 52, no. 14, pp. 88–93, Jan. 2019, doi: 10.1016/j.ifacol.2019.09.169.

[39]   "What Is a Process Model? - MATLAB & Simulink - MathWorks United Kingdom." https://uk.mathworks.com/help/ident/ug/what-is-a-process-model.html (accessed Dec. 06, 2021).

[40]   S. Abouelazayem, I. Glavinić, T. Wondrak, and J. Hlava, "Switched MPC Based on Clogging Detection in Continuous Casting Process," *IFAC-PapersOnLine*, vol. 53, no. 2, pp. 11491–11496, Jan. 2020, doi: 10.1016/j.ifacol.2020.12.589.

[41]   R. Aguilera, P. Lezana Illesca, and D. Quevedo, "Switched Model Predictive Control for Improved Transient and Steady-State Performance," *Industrial Informatics, IEEE Transactions on*, vol. 11, pp. 968–977, Aug. 2015, doi: 10.1109/TII.2015.2449992.

[42]   L. Zhang and R. D. Braatz, "On switched MPC of a class of switched linear systems with modal dwell time," in *52nd IEEE Conference on Decision and Control*, Dec. 2013, pp. 91–96. doi: 10.1109/CDC.2013.6759864.

[43]   S. Abouelazayem, I. Glavinic, T. Wondrak, and J. Hlava, "Adaptive Control of Meniscus Velocity in Continuous Caster based on NARX Neural Network Model," *IFAC-PapersOnLine*, vol. 52, pp. 222–227, Jan. 2019, doi: 10.1016/j.ifacol.2019.12.653.

[44]   S. Abouelazayem, I. Glavinić, T. Wondrak, and J. Hlava, "Flow Control Based on Feature Extraction in Continuous Casting Process," *Sensors*, vol. 20, no. 23, Art. no. 23, Jan. 2020, doi: 10.3390/s20236880.